FLEXURAL BEHAVIOR OF OVER REINFORCED HSC BEAMS CONFINED BY RECTANGULAR TIES

Abdou Khalaf Mohamed[(b)], A. S. Elamary[(b)], M. M. Ahmed[(a)]

[(a)] *Department of Civil Engineering, Assiut University, Assiut, Egypt*
[(b)] *Department of Structural Engineering, Alazhar University, Kena, Egypt*

This paper presents an experimental and analytical investigation on the flexural behavior of over reinforced concrete beam confined by rectangular ties. The experimental investigation was conducted through testing four full-scale beams with normal strength concrete (NSC). Three out of these four beams were confined using rectangular ties located on the compression region of the beams. The variables studied in these specimens were the volumetric ratio of transverse reinforcement, and the volumetric ratio of the main rebars. A finite element model was established with both material and geometrical non-linearity by using ANSYS software package. Accuracy of the model was assessed by applying it to the three tested beams. Comparison of analytical results with the available experimental results for ultimate load values and load–deflection relationships show a good agreement between the finite element and experimental results. After validating the accuracy of the proposed model, parametric study was undertaken to gain additional insight into the overall behaviour, failure modes, and deformation capacity for the concrete beams using high class concrete strength. The parameters studied were, the concrete compressive strength, the number and diameter of longitudinal rebars, and diameter of rectangular ties. The obtained results show that, the strength and ductility of high strength concrete (HSC) beams are enhanced through the application of rectangular tie reinforcement located in the compression region of the beams. The concrete compressive strength, the longitudinal bars number and diameter, and the diameter of rectangular ties are important parameters controlling the level of strength and ductility enhancement of over-reinforced HSC beams.

AUTHOR KEYWORDS: *High-strength concrete; confined concrete beam; flexural behavior*

1. INTRODUCTION

The development of the construction industry has led to the continual improvement of construction materials where high strength concrete (HSC) of 100 MPa compressive strength and reinforcement of 500 MPa yield strength are used in beams and other construction members. High-strength concrete is now readily available for various practical applications such as bridges, offshore platforms and buildings, as a result of ongoing progress in concrete technology. Higher strength of materials is usually

associated with a decrease in the ductility of the materials compared to their lower strength counterparts. HSC offers many advantages, including excellent mechanical performance and durability, which could lead to an initial and long-term cost reduction. HSC, however, is more brittle than conventional normal strength concrete (NSC). Current confinement requirements [5], which were originally derived from experimental results on NSC, are not suited for HSC elements [2 and 18]. In recent years, there has been some concern about the use of HSC in building columns in seismic areas and as a consequence, the application of HSC in high seismic regions has lagged behind its application in regions of low seismicity. Seismic-resistant design of reinforced ductile frame buildings [23], provides the mandate condition of a strong column and weak beam at any junction. The intent is to encourage hinging in the beams rather than in the columns. However, building performance during seismic activity indicates that hinging can occur in columns. Therefore, the possibility of plastic hinge formation at column ends demands that building columns in seismic areas must have sufficient ductility. More and over, that was one of the mean reasons to open a research area on studying HSC beams. This investigation was conducted to examine the flexure behavior of over reinforcement HSC beams confined by using rectangular ties. The beams were subjected to two points load, where the variables studied were the volumetric ratio of longitudinal reinforcement, tie configuration and tie yield strength.

NOMENCLATURE

A_s	area of longitudinal bars	f_y	yielding stress of longitudinal reinforcement
A_{sc}	area of longitudinal top bars		
d'	nominal diameter of lateral ties	f_{yh}	yielding stress of longitudinal reinforcement
d	nominal diameter of longitudinal steel bars	h'	length of one side of rectangular tie
E_s	modulus of elasticity of reinforcing steel	n	number of longitudinal steel bars
f_u	ultimate strength of reinforcing steel	S	centre-to-centre spacing of lateral ties
f'_c	cylindrical compressive strength of concrete specimen	ρ_{max}	maximum volumetric ratio of transverse reinforcement
f'_{cu}	cube compressive strength of concrete specimen	ρ_s	volumetric ratio of lateral reinforcement

---

2. LITERATURE REVIEW AND THEORETICAL BACKGROUND

Hadi and Schmidt [13] tested seven high strength concrete (HSC) beams helically confined in the compression zone, all beams had the same helical pitch of 25 mm to study different variables excluding the helical pitch. However, the literature indicates the importance of helical pitch, but there is no quantitative data for over-reinforced helically confined HSC beams. Shin et al. [22] tested 36 beams, four of those were to study the effect of tie spacing on ductility. The results did not show clearly the effect of confinement spacing. It may be because the spacing studied was only 75 and 150 mm

which did not provide adequate data to figure out the importance of confinement spacing. Sheikh and Uzumeri [19] examined the effect of different variables on the behavior of the strength and ductility of columns by testing 24 specimens. The results pointed out to the significant influence of the helical pitch on the behavior of confined concrete.
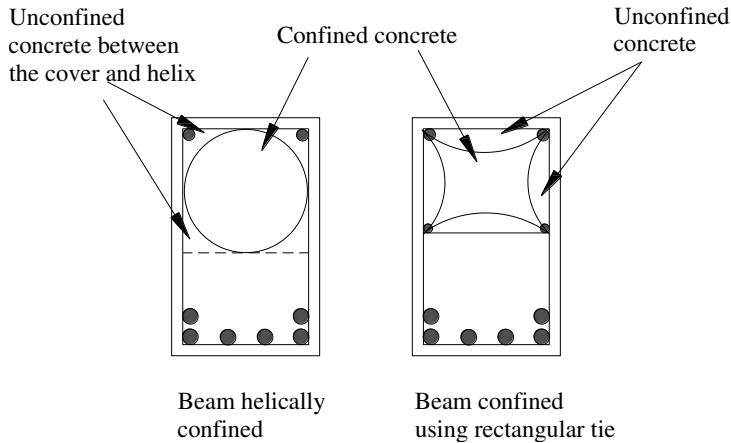

Fig. 1. Confined and unconfined compression concrete in beams.

Hatanaka and Tanigawa [6] stated that the lateral pressure produced by a rectangular tie is about 30–50% of the pressure introduced by a helix. That will be the case for compression concrete in columns or beams. However, helix confines the concrete more effectively than rectangular ties because helix applies a uniform radial stress to the concrete along the concrete member, whereas a rectangular tie tends to confine the concrete mainly at the corners. Using helical confinement in the compression zone of rectangular beams is more effective than rectangular ties even though there is a very small portion of compression concrete that is not confined. This area is at the corner as shown in Fig.1. However, that is proved experimentally that the helix is more effective than the rectangular ties for NSC by [15]. The comparison between the effect of helix with rectangular confinement of over reinforced concrete beams using the experimental data of Mansur et al. [17] and Ziara et al. [12] was very difficult because of different variables such as size and span of the beam, tie spacing and longitudinal reinforcement ratio. The comparison between the effectiveness of helix and tie in the compression zone of HSC beams will be undertaken during the next stage of the extensive experimental program at the University of Wollongong [15].

Several empirical models [20, 24] have been proposed to model the stress strain curve for confined HSC. The following is a brief description of the model presented by Yong et al [24]. Based on experimental data, Yong et al. [24] have proposed the following equations to predict the peak compressive stress f_o and corresponding compressive strain ε_o for confined HSC.

$$f_o = Kf_c^{'} \tag{1}$$

Where

$$K = 1 + 0.0091\left[1 - \frac{0.245S}{h'}\left(\rho_s + \frac{nd'}{8Sd}\rho\right)\frac{f_{yh}}{\sqrt{f_c'}}\right] \qquad (2)$$

An expression for ε_o as follows

$$\varepsilon_o = 0.00265 + \frac{0.0035\left(1 - (0.734S/h')\right)\left(\rho_s f_{yh}\right)^{2/3}}{\sqrt{f_c'}} \qquad (3)$$

The remaining unknown values were calculated using equations obtained by linear regression and shown in details in [20-24] where the units used in the above equations are in N, mm.

3. EXPERIMENTAL PROGRAMME

The aim of the experimental program in this study was from one hand to investigate the behavior of over-reinforced NSC beams confined using rectangular tie; and to determine the effect of additional rectangular ties on their strength and ductility, from the other hand to verify the theoretical results. The number of longitudinal rebars and concrete compressive strength were the only parameters selected for investigation in the current experimental programme.

3.1. Specimens

Four over-reinforced concrete beams with a rectangular cross-section of 150 mm width and 230 mm height were tested under two points loading. The tested beams performed over a simple span of 2200 mm and a shear span to depth ratio equal 4. The beam effective depth was 210 mm, generic details of the beams are shown in Fig. 2. The specimens were designed to ascertain the flexural strength and ductility enhancement in over-reinforced concrete beams. The concrete mix designed to produce a cube compressive strength 250 kg/cm2 after 28 days. The mix component ratios will be indicated in the upcoming section. Three out of the four beams were provided by rectangular steel ties in the compression zone. The confined beams nominated as Bst1, Bst2, and Bst3, with four, six and eight 16 mm diameter, longitudinal reinforcement bottom bars, respectively. Two 10 mm plain bars were installed at the top of the beams in order to keep the stirrups in-place. The beams had two types of stirrups which made of 8 mm and 6 mm plain bars. The main stirrups 8 mm diameter were performed for full beam depth and at a spacing of 100 mm, in additional to a short rectangular stirrups of 6 mm diameter at a spacing of 100 mm applied in the compression zone of beam, staggered with the main stirrups, as shown in Fig 2. The fourth beam Bst4 had the same geometric and steel reinforcement of Bst2 but without confinement (6 mm stirrups). The dimensions and steel-bar-reinforcement layout of the reinforced concrete beams are shown in Fig. 2. The details of the test specimens are reported in table 2. Each specimen contained different number of longitudinal bars providing a different reinforcement ratio. The volumetric ratio of transverse reinforcement to concrete core, measured centre-to-centre of perimeter ties, were varied between 1.58% and 2.25%.
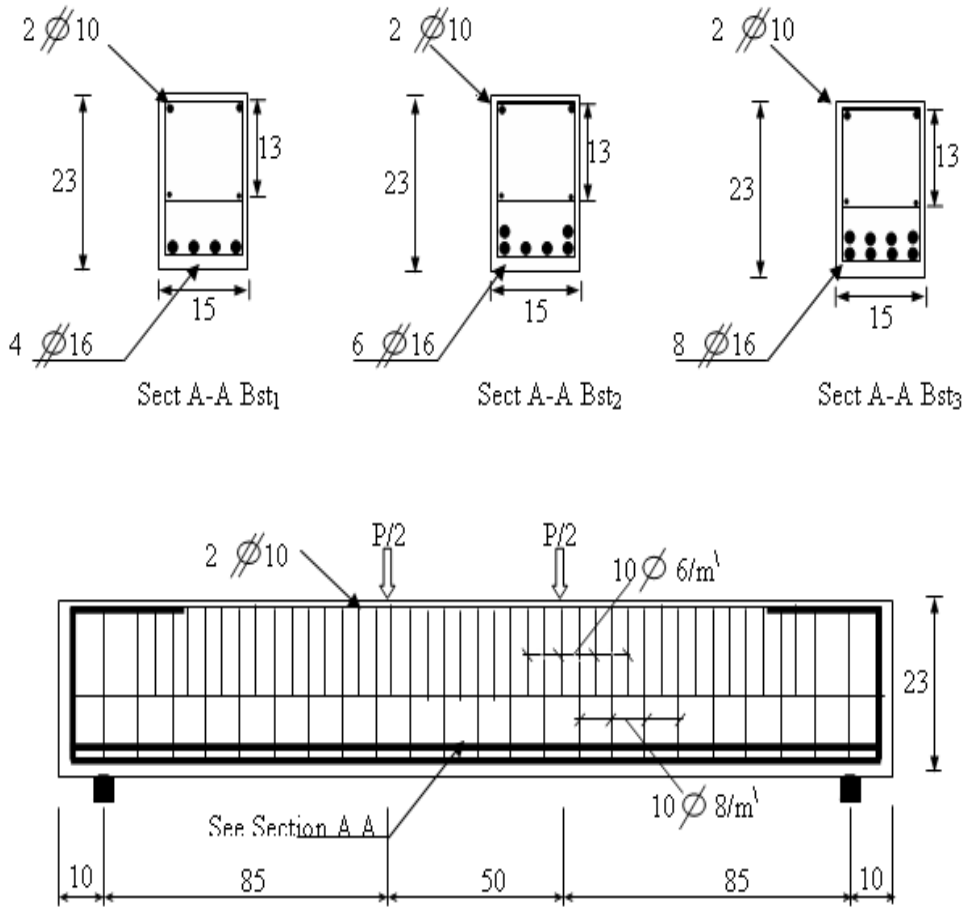
Fig. 2. Detail of specimens (unit: cm).

3.2. Materials

The concrete mix was designed to produce 250 kg/cm2 strength of cube concrete 28 days. The mix proportions by weight were 350 kg cement, 603 kg sand, 1207 kg gravel, and 192 liter of water. The measured compressive strengths of concrete cubes at the date of testing are listed in Table 1. Two different types of reinforcing steel were used to construct specimens as shown in Fig.2. Important properties of steel are also listed in Table. 2. The parameters f_y and f_u represent the yield or proof and ultimate strength of the steel bars, respectively.

3.3. INSTRUMENTATION AND TEST PROCEDURES

All beams were tested at age of 28 days using the same test procedures and instrumentation. All beams were instrumented using stain gauges and dial gauges. Reinforcement steel deformation was measured using electrical-resistance strain gauges (20 mm length) glued to the steel bars at mid-span of the bar. The mid-span

deflection of the beam was measured using dial gauges with an accuracy of .01 mm. These dial gauges were placed on the beam bottom surface at mid-span. All the data were recorded using Smart System installed in a PC computer. Test setup and loading conditions are shown in Fig 3.a. The initial reading of the dial gauge was first recorded. The test began with application of the load to the target value incrementally. For the first step of loading, the load value was 1.4 ton, where the next steps of loading increments were 0.5 ton until final collapse of the beams. The load was kept constant between two successive increments for about 3 minutes, to enable recording of the different readings, and observing the cracks. All the experimental data were stored at predetermined steps and recorded at special occurrences such as cracking, and ultimate displacement. Mid-span deflection versus applied load obtained from each beam are shown schematically in Fig 3-b.

Table 1: Details of tested beams:

Beam No.	f_{cu} kg/c m^2	A_s	ρ %	ρ_{max} %	A_{sc}	spacing between short stirrups (cm)	Volume of short stirrups (V_{st}) cm^3/cm
Bst$_1$	265	4Φ16	2.82	1.32	2Φ10	10	1.47
Bst$_2$	220	6Φ16	4.23	1.1	2Φ10	10	1.47
Bst$_3$	265	8Φ16	5.64	1.32	2Φ10	10	1.47
Bst$_4$	265	6Φ16	4.23	1.32	2Φ10	-	-

Table 2. Properties of reinforcement

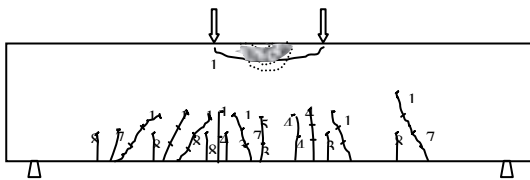| Properties	Diameter of re-bars (mm)			
	Φ6	Φ8	Φ10	Φ16
Yield or proof strength (f_y) kg/cm^2	3222	3890	4711	4376
Ultimate strength (f_u) kg/cm^2	4476	5128	6875	7261
Elongation %	33.75	32.04	30	21.8

a- Test set up
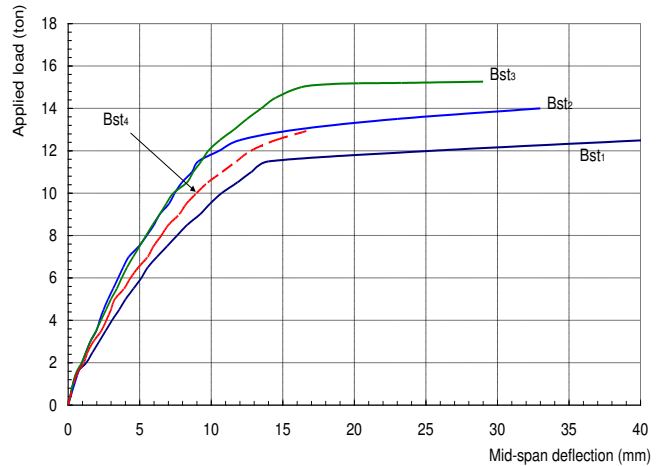
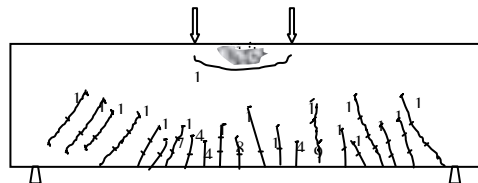b- Mid-span deflection vs applied load for tested beams

Fig 3. Test set up and tests results

4. TEST RESULTS

4.1. Test observations

a- Pattern of cracks for beam (Bst2)

b- Pattern of cracks for beam (Bst3)

c- Shape of failure of beam (Bst2)

d- Shape of failure of beam (Bst3)

Fig 4. Cracks pattern and shape of failure.

The first cracks initiated at the bottom fibers in the constant moment zone. After these cracks, by increasing the applied load another inclined cracks appeared and the formed

cracks propagated towards the point of load application as shown in Fig. 4. Such a cracks height was greater for beam Bst1 (ρ = 2.82) more than that of beam Bst2 (ρ = 4.23) and beam Bst3 (ρ = 5.64), as shown in Figs 4.c and 4.d. The rate of crack propagation was smaller than that of the reference beam Bst4 without any confining. This could be show the confining effect of short rectangular stirrups. Prior to failure a horizontal crack was initiated near the upper side of these beams at the steel level and the concrete cover began to spall off as shown in Fig. 4. The modes of failure changed from a brittle flexural compression to a ductile flexural compression through crushing in the compression zone in a gradual manner and buckling of upper steel.

4.2. DISCUSSION OF RESULTS

The relation between the total applied load and the measured mid-span deflection for the four tested beams is illustrated in Fig 3-b. Through this figure it is noticed that, the presence of short rectangular stirrups in over reinforced NSC beams enhance their deformability and hence ductility. The length of the flat Plato of the curves for the confined beams showed a considerable increase. The effectiveness of the short rectangular stirrups is dependent on the degree of over reinforcing and the volume of the used short rectangular stirrups. The confined beam Bst1 with a smaller degree of over reinforcing recorded a greater deflection at various load level. Although the deflections for beams Bst2 and Bst3 at any load level up to ultimate load (P_u) for beam Bst4 were almost similar and smaller than the unconfined beam Bst4 as shown in Fig 3-b [3]. However the deflection of these beams corresponding to load greater than 0.8 P_u was bigger than the corresponding value of the reference beam Bst4. This can be attributed to two evidences; the first was the concrete compressive strength of beam Bst2 and the higher degree of over reinforcing in beam Bst3, where the second was the fact that the effect of confining is more activated at higher load level. It was also noticed that, as the longitudinal reinforcement ratio increases the ductility index decreases, hence more confining force is required to develop large deformability. The displacement ductility index for beam Bst1 having 2.82% longitudinal reinforcement ratio is more than both the corresponding value in beam Bst2 having 4.23% longitudinal reinforcement ratio (103.9%) and in beam Bst3 having 5.64% longitudinal reinforcement ratio (107.2%). This also indicates the brittle behavior for beams having higher percentage of longitudinal reinforcement. Furthermore the reduction in ductility index for these beams was approximately linearly proportional with the increase in the amount of tension reinforcement.

5. FINITE ELEMENT ANALYSIS

5.1. General

The finite element analysis will be used in the numerical analysis in this paper by conducting a numerical model represented only a half of the full beams size performed and tested at the University of Assiut by Abd-Elkader   et   al.   [3].   The   symmetry boundary conditions were used at the beam center in order to simulate the full beam adequately as shown in Figures 5 and 6-a.
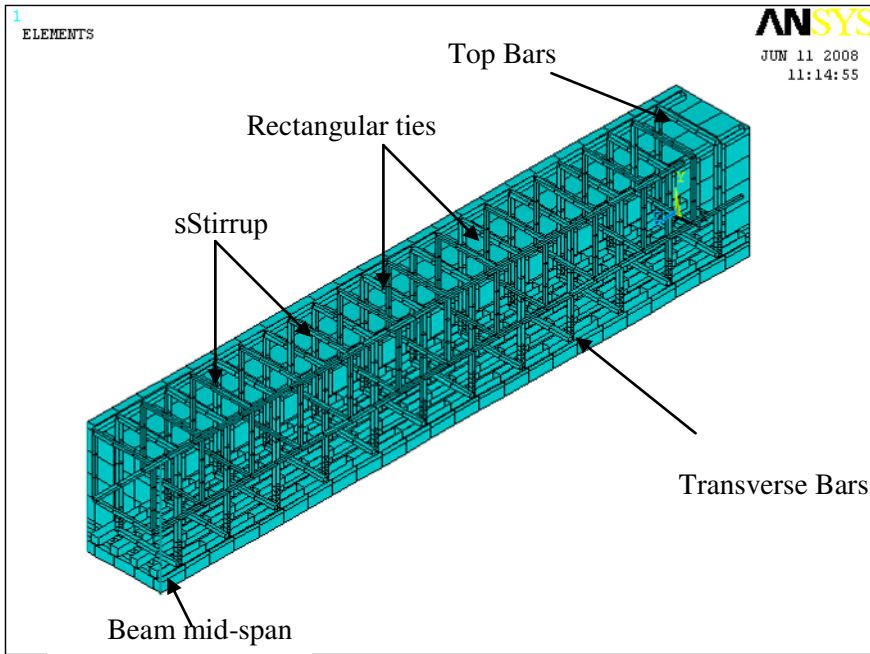
Fig. 5 Modelling of reinforcement re-bars elements.

The boundary conditions of the FE model aimed to simulate the actual boundary conditions of the tested beams. The load applied at the top of the beam in two positions as concentrated loads similar to the load points condition applied in the test as shown in Fig 6-a. The out of plane displacement of the loaded points were restrained to prevent the lateral torsional effect. Using the ANSYS finite element software, a three dimensional solid finite element model was constructed. The program provides a dedicated three dimensional eight nodded solid isoparametric element, Solid65, to model the nonlinear response of brittle materials based on a constitutive model for the triaxial behavior of concrete after Williams and Warnke (1974). The element includes a smeared crack analogy for cracking in tension zones and a plasticity algorithm to account for the possibility of concrete crushing in compression zones. Each element has eight integration points at which cracking and crushing checks are performed. The element behaves in a linear elastic manner until either of the specified tensile or compressive strengths is exceeded. Cracking or crushing of an element is initiated once one of the element principal stresses, at an element integration point, exceeds the tension or compressive strength of the concrete. Cracked or crushed regions, as opposed to discrete cracks, are then formed perpendicular to the relevant principal stress direction with stresses being redistributed locally. The amount of shear transfer across a crack can be varied between full shear transfer and no shear transfer (0.0) at a cracked section. The smeared stiffness and strut modeling options allow the elastic-plastic response of the reinforcement to be included in the simulation at the expense of the shear stiffness of the reinforcing bars. In this case the reinforcement modeled using strut elements Link8. These elements are embedded in the mesh of solid65 elements and the inherent assumption is that there is a perfect bond between the reinforcing bars and the surrounding concrete. A linear elastic perfectly plastic

material law, described by the elastic modulus, the yield strength and the post-yield stiffness of the material, was used for these elements.

5.2. Model Verification

Finite element (FE) models executed for the three confined beams Bst1, Bst2, and Bst3 to verify the performance of the model shown in Fig 6-a. Mid-span deflection versus applied load curves obtained from the FE models of Bst1, Bst2, and Bst3 plotted in Fig 6- b, c, and d respectively and compared with the experimental results. The comparison shown in these figures confirmed that the FE models can represent the beams to an acceptable degree of accuracy. In order to have not any suspicious about the FE models, the final horizontal, vertical, and inclined cracks shape resulted from the experimental compared with the FE model as shown in Fig. 7.
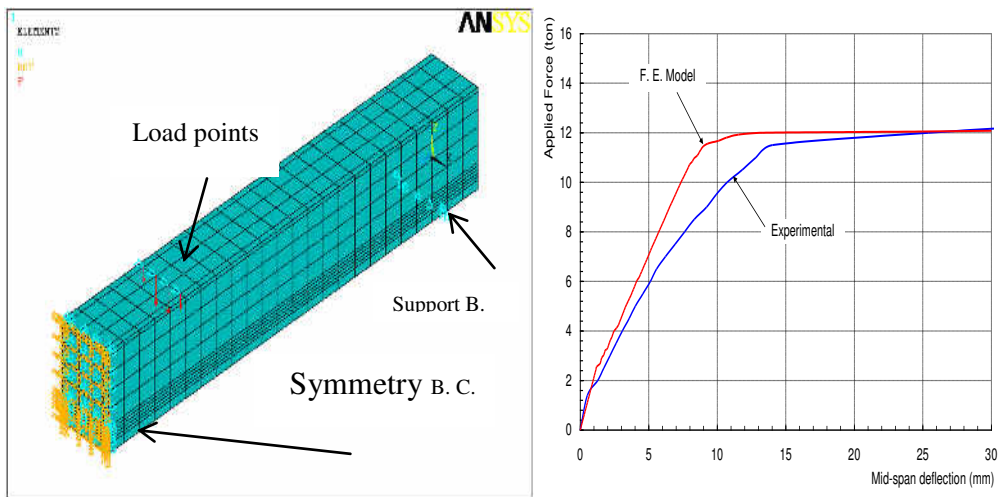
a- Finite element model - boundary conditions   b- Experimental and FE model results -Bst1
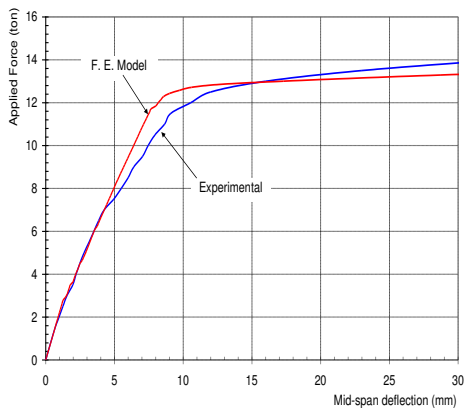
c- Experimental and FE model results - Bst2   d-Experimental and FE model results -Bst3
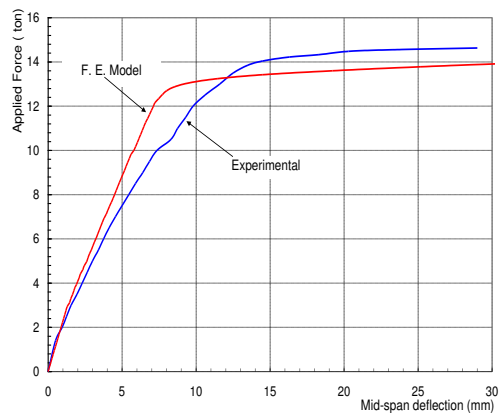
Fig.6 Comparisons between experimental and FE models results.

Based on these models the effect of concrete compressive strength and the transverse bars, number and diameter, were studied on the flexure behavior of HSC beams confined by using rectangular ties. Before start these analyses, it should be mentioned that, since there isn't available information about the maximum allowable percentage of main steel for the HSC, consequently, the maximum allowable was calculated using the percentages stated in table 4-1 of the Egyptians code [9] for NSC. This percentage based on the yield and ultimate strength of the main reinforcement which corresponding to ($3.65\ E\text{-}4\ *\ F_{cu}$) in this case.
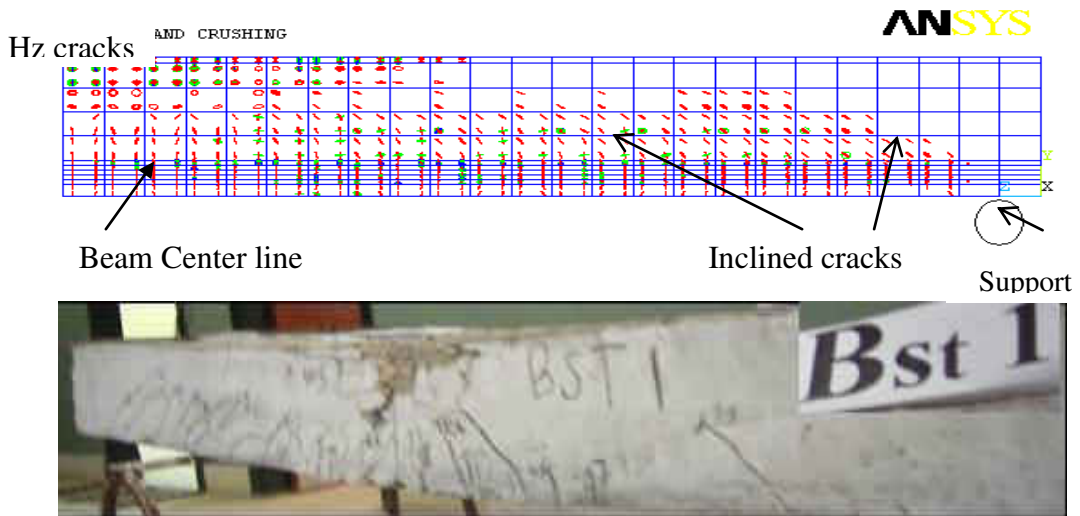
Fig.7 Comparisons between experimental and FE models cracks results.

6. PARAMETRIC ANALYSES

As mentioned previously, the effects of four variables were investigated in the present analytical programme: (1) concrete compressive strength; (2) the volumetric ratio of transverse steel; (3) rectangular ties diameter; and (4) the longitudinal steel configuration. It is possible to assess the effect of each variable graphically from Fig 8 to Fig 13. To quantify the response of the beams, it is desirable to define response indices that quantitatively describe the beams' behavior. In seismic design as one of the most critical design process, the elastic deformation is generally quantified by ductility parameters and by energy dissipation capacity. For long-period structures, it has been stated that ductility is directly related to the strength reduction factor used in most codes [17] to calculate the seismic base shear. Deflection ductility index is defined as the ratio of ultimate deflection to the yield deflection. The energy dissipation capacity is an important parameter in the design of short-period structures and structures subjected to a long-duration earthquake. For simplicity the energy dissipation can be defined by the area under the load deflection curve up to 80% of ultimate strain. In this investigation the ductility index and the ultimate force achieved will be used as the basis of comparison the flexural behavior of the analyzed beams. Consequently, the results comparison for each parameter will be concerned with the ductility factor and energy dissipation.
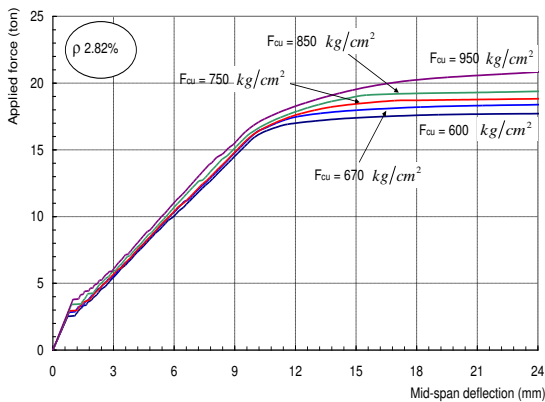
6-1 Effect of Concrete Compressive Strength

As shown in table 3, five different class of concrete; 600, 670, 750, 850, and 950 kg/cm^2 were used to study the effect of concrete compressive strength in the three beams Bst1, Bst2, and Bst3. The diameter of the main longitudinal bars was 16 mm, where the beams were confined using 6 mm rectangular ties in the beams compression zones. Fig. 8-a, shows the behavior of Bst1, based on this finding, it can be concluded that the deflection ductility index did not affect significantly by the class of concrete when the HSC beam has low ratio of steel. While the load deflection area regarding to the energy dissipation show a little increase. The percentage of increase in the ultimate load capacity of that beam ranged from 4% to 20% referenced to 600 kg/cm^2 concrete compressive strength. Beam Bst2 with a percentage of longitudinal bars equal 4.23% show different yield deflection in each class of concrete with almost equal ultimate deflection; which means that the deflection ductility index decreased by increasing the class of concrete as shown in Fig.8-b. On the other hand, the area of energy dissipation is increased significantly in this beam by applying higher class of concrete.

Table 3. List of Parameters studied

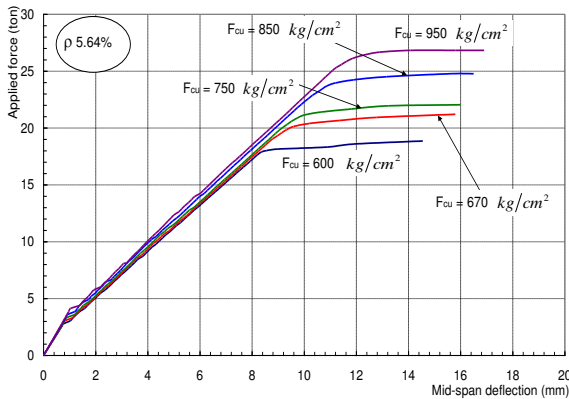| Parameter	Beam No.	Concrete compressive strength (kg/cm2)	Longitudinal rebar		Diameter of additional Rec. ties (mm)
			No.	Diameter (mm)	
Concrete Compressive strength	Bst1	600, 670, 750, 850, 950	4	16	6
	Bst2	600, 670, 750, 850, 950	6	16	6
	Bst3	600, 670, 750, 850, 950	8	16	6
Longitudinal rebar	Bst1	600	4	16, 18, 22	6
	Bst2	600	6	16, 18, 22	6
	Bst3	600	8	16, 18, 22	6
Additional rectangular ties	Bst1	600	4	16	6, 8, 10
	Bst2	600	6	16	6, 8, 10
	Bst3	600	8	16	6, 8, 10

The ultimate load capacity of this beam increased higher than Bst1; and the percentage of increased ranged from 6% to 35% referenced to 600 kg/cm^2 concrete compressive strength. The behavior of the third beam Bst3 with $\rho = 5.64\%$; shown in Fig. 8-c. From this figure it can be noticed that the percentage of deflection ductility index had a minor decrease due to increase in the yield deflection position with relevant increase in the ultimate deflection. The ultimate load capacity increased significantly and ranged from 10% to 40% from the ultimate load obtained by using 600 kg/cm^2 concrete compressive strength as a reference.

a- Bst1–different concrete compressive strength
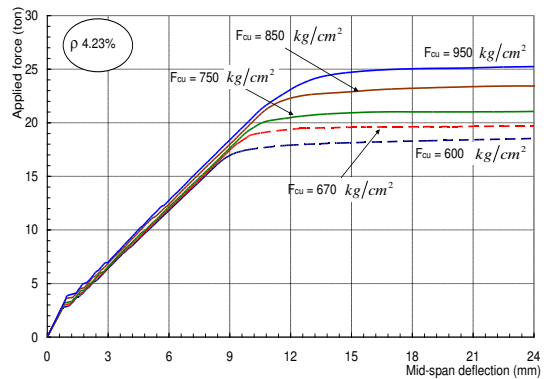
b- Bst2–different concrete compressive strength


c- Bst3 - different concrete compressive strength
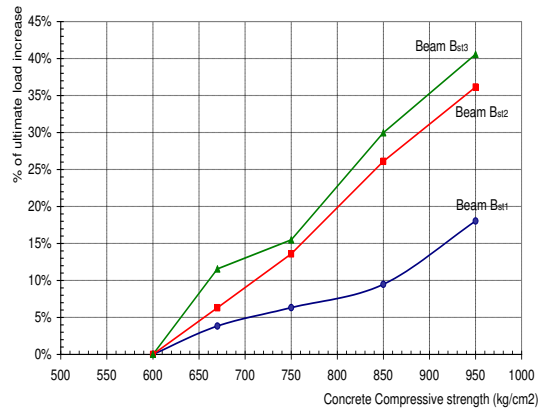
d- Effect of concrete compressive strength

Fig.8-Load versus mid span deflection for beams with concrete compressive strengths
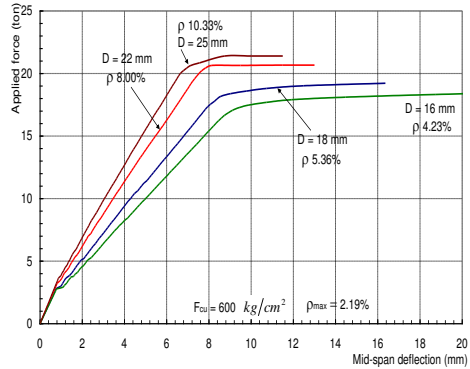
6-2 Effect of Longitudinal Main Bars Diameter

The effect of steel configuration on the behavior of HSC beams can be examined by comparing the behavior of FE models results for Bst1, Bst2, and Bst3 as shown in table 3 and Fig. 9-a, b, and c. The three analyzed beams had a concrete compressive strength 600 kg/cm^2 with maximum allowable percentage of transverse re-bars equal $\rho_{max} =$

2.19% as stated in Egyptian codes [9]. Each beam had a different numbers of longitudinal rebars as abovementioned and confined using 6 mm rectangular ties. The four diameter sizes which studied in this section for each beam were 16 mm, 18 mm, 22 mm, and 25 mm. The results obtained from these analyses plotted in Fig. 9 a, b, and c. Finally a comparison between the percentages of increase in the ultimate load capacity versus the bars the longitudinal bars diameter is plotted in Fig. 9-d.\
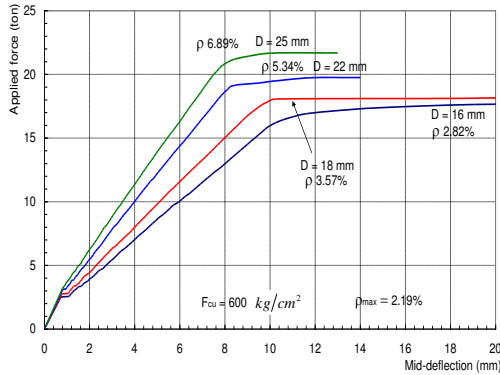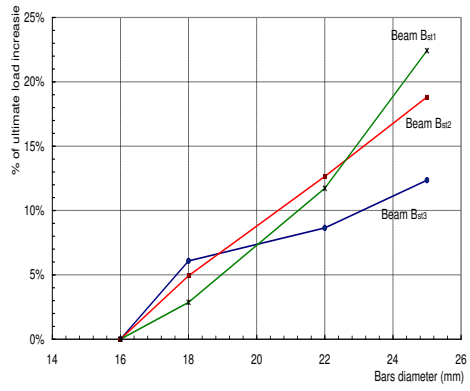

a- Bst1 – Effect of main rebars diameter

b- Bst2- Effect of main rebars diameter
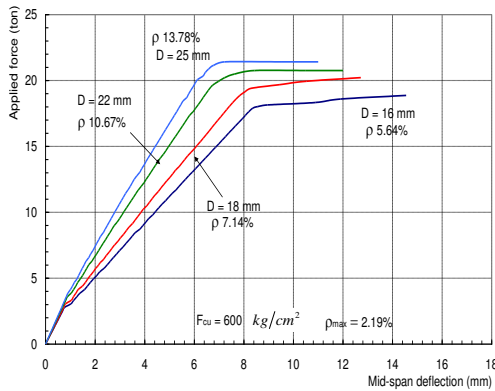
c- Bst3 - Effect of main rebars diameter

d- Percentage of increase in ultimate load.

Fig. 9- Load versus mid span deflection for different diameter of longitudinal rebars.

Bst1 shows a higher deflection ductility index by using diameters 16 mm and 18 mm with a percentage ratio ρ = 2.82% and 3.57% respectively as shown in Fig. 9–a. In the same figure when the diameter increased to 22 mm and 25 mm the initial stiffness increased significantly on the other hand the deflection ductility index decreased in both cases due to increasing the yield deflection.

Figure 9-b shows the behavior of Bst2 which had six transverse bars. In this beam the analyses performed for 16, 18, 22, and 25 mm diameters of re-bars, equivalent to ρ equal 4.23%, 5.36%, 8%, and 10.33% respectively. The results obtained plotted in this figure shows that the initial stiffness has a direct proportional with the percentage of the longitudinal bars diameter where the contrary obtained in the ultimate deflection achieved be the beam which means decreasing in the ductility index.

By increasing the number of longitudinal bars to eight as performed in Bst3 the behavior of the beam changed significantly as shown in figure 9-c. In this beam the ρ was equal 5.64%, 7.14%, 10.67%, and 13.78% by using 16 mm, 18 mm, 22 mm, and 25 mm diameter respectively. The same notices obtained, which stated for Bst2 except that the deflection ductility index had a small value for all cases.

Regarding to the percentage of increase in the ultimate load capacity, the three beams compared by using the first diameter 16 mm as a reference of these percentage of increase. Fig. 9-d shows the percentage of increase on the ultimate load capacity for each beam, Bst2 shows gradual increase represented by linear curve started from 5% to 18% corresponding to 18, and 25 mm diameter respectively.

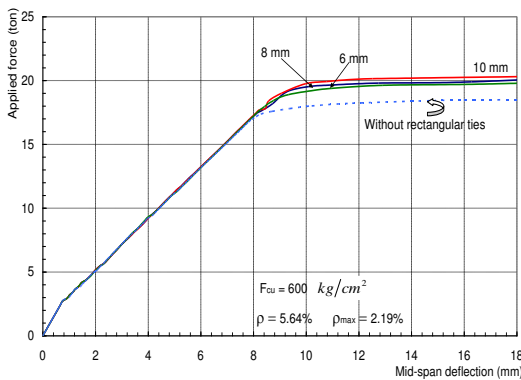## 6-3 Effect of rectangular tie diameter

The three analyzed beams Bst1, Bst2, and Bst3 had a concrete compressive strength 600 kg/cm^2. Each beam had a different numbers of longitudinal rebars as abovementioned and listed in table 3.
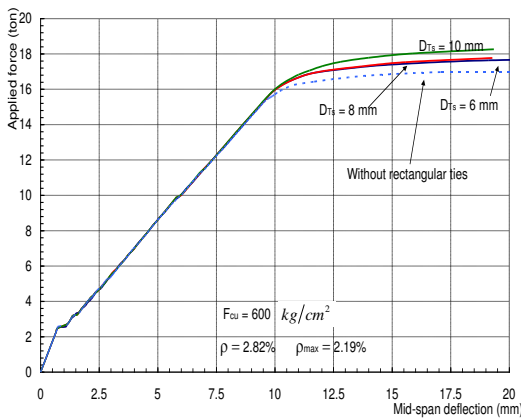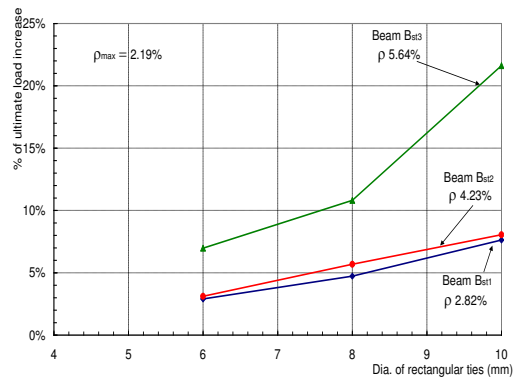

a- Bst1- Without and with (6, 8, 10 mm) rect. ties
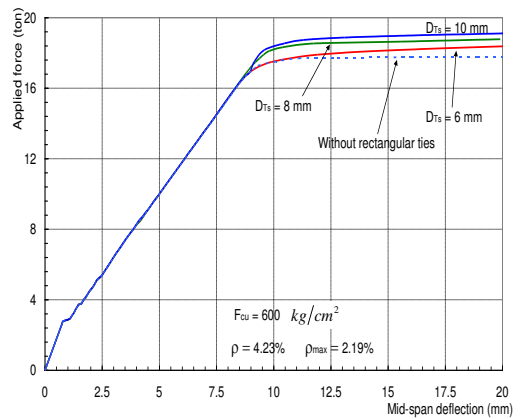
b- Bst2-Without and with (6, 8, 10 mm) rect. ties

c- Bst3 - Without and with (6, 8, 10 mm) rect. ties

d- percentage of increased in ultimate capacity

Fig. 10- Load versus mid span deflection for different rectangular ties diameter.

The effect of rectangular ties diameter was studied by comparing the flexural behavior of each beam without ties with the same beam confined by using 6 mm, 8 mm, or 10 mm diameter of rectangular ties. The results obtained from these comparisons plotted in Fig. 10-a. b. and c. The confinement had not any effect on the initial stiffness where it had a significant effect on the ultimate capacity of each beam as shown in Fig. 10-d. Using the unconfined beam as a reference, the ultimate capacity of beams Bst1 and Bst1 with ρ equal 2.82% and 4.23% respectively had an increased ranged from 3% to 8% maximum Fig 10-d. Where, for beam Bst3 with ρ equal 5.64% had higher increase in the ultimate load ranged from 7% to 23% as shown in Fig 10-d.

6-4 Effect of Number and Position of Longitudinal Main Bars

To gain further insight into the flexural behavior of HSC beams and point out the percentage of longitudinal steel which can be consider as a maximum percentage the number of main bars studied herein. The three confined beams Bst1, Bst2, and Bst3 with a concrete compressive strength 600 kg/cm^2 and under two points load were analyzed.

The same volumetric ratio of confinement steel is assessed on the three set of beams studied. In the initial stage of loading process the three beams show the same behavior, where the bottom surface of concrete located in the maximum moment zone start to be cracked at earlier stage of load, almost from 15% to 20% of ultimate load achieved, as shown in Fig.11. From this figure it can noticed that the concrete can carry a maximum 10% from the total tensile force which generated by the bending moment action. After that value the concrete zone subjected to tension is completely cracked and can not sustain any additional load, consequently, beam tensile resistance after this value based only on the main bars. A ductile failure can be consider if these bars reach its yield strength without occurring sudden beam failure. Fig. 12-a. shows the results obtained from Bst1 using four bars 18 mm diameter. It is noticed that, by using (ρ 3.57%) ductile failure performed; where if the beam with ρ equal to 6.9% the ductility index decreased 25% as shown in Fig 9-a.
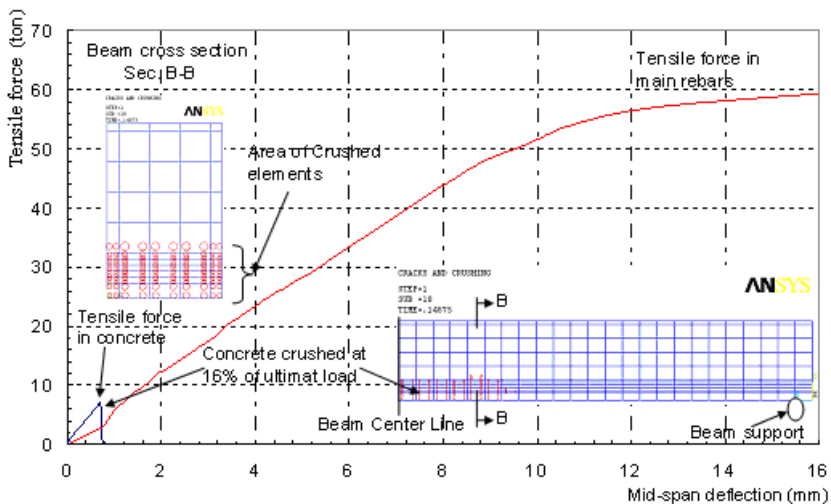

Fig. 11 Beam Bst2 – concrete and re-bars tensile force - Concrete crushed area

Figure 12-b, shows the mid span deflection versus longitudinal bars tension force regarding to the confined beam Bst3 with concrete compressive strength 600 kg/cm^2. It is noticed that, the only ductile failure obtained with ρ equal 5.64% (16 mm), where all the rest show brittle failures.

The number of longitudinal bars effect can be released from Figs. 8-d, 9-d, and 10-d. These figures compared the percentages of increase in the ultimate load achieved by the three beams. From these figures, it is seen that, the beam Bst2 was representing the average and the best performance. Herein it can be concluded that, the percentage of longitudinal bars is not the only factor that affect the performance of the beam but also the positions of the bars.
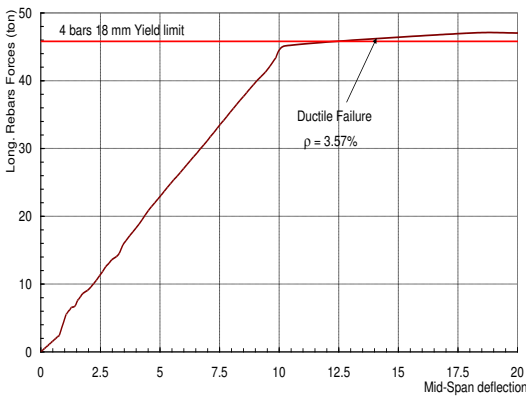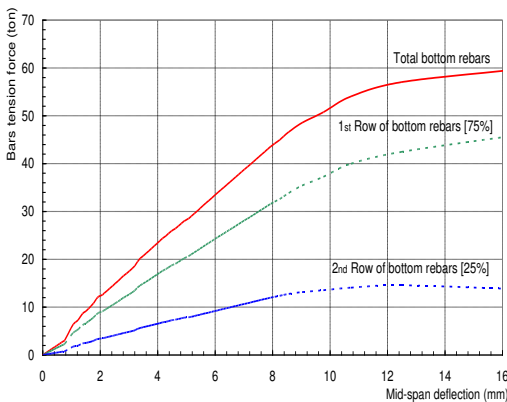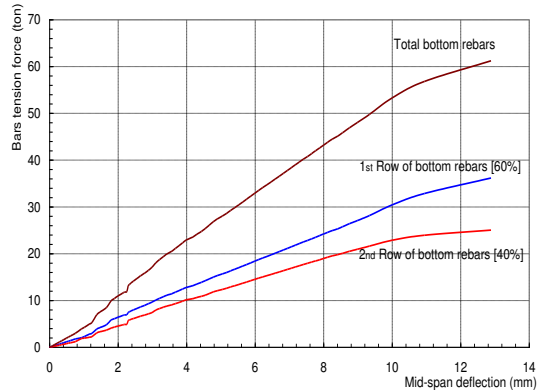

a- Beam Bst1 – ductile failure
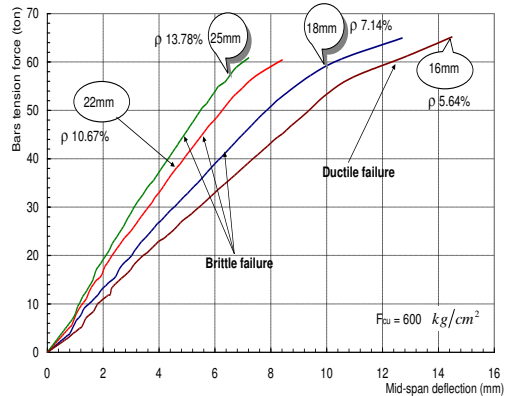
b- Beam Bst3 - Ductile and brittle failures.

Fig. 12 Failure modes in Bst1 and Bst3

Beam Bst2 –Tensile force in each row of steel

Beam Bst3 -Tensile force in each row of steel

Fig. 13 Longitudinal bars- participation of each row in the total tensile force

In order to deeply understand the benefits which can be gained due the bars arrangement, the total tensile force generated in the main longitudinal bars in beams Bst2 and Bst3 are shown in Fig. 13 a. and b. The contributions of each row of these bars from the total force generated by the bending moment action are different and

depend on the number of bars in each row. Fig. 13-a. shows the percentage of participation of each row from the total tensile force for beam Bst2, with six bars, four in the first row (75%) and two in the second (25%). The percentage of the forced transferred by each row is complete different in Beam Bst3, with eight bars, four in each row (60%, and 40%). The results also indicate that, the yield and the ultimate strengths of longitudinal reinforcement have a significant effect on the ultimate capacity of the HSC beam, which are not considered in the confinement model of HSC beam Eqs. 1, 2, and 3 presented by Yong et al. [24]. More and over the number of the longitudinal bars has a significant effect of the ultimate capacity where it has a minor effect in Eqs. 2 proposed by [24].

7. CONCLUSIONS

The experimental program in this study was to investigate and provide experimental evidence about the significant effect of rectangular ties on the behavior of NSC beam. Three over-reinforced HSC beams confined by using rectangular ties were tested. Finite element models were conducted and the results compared with the experimental output data obtained. The comparisons show that the FE models can represent the beams to a good degree of accuracy. Parametric studies were executed on these models to study the effect of concrete compressive strength, rectangular ties diameter, and transverse bars configurations. Conclusions can be drawn about the behavior of these HSC beams as follow:

- The concrete compressive strength, the transverse bars number and diameter, and the diameter of rectangular ties are important parameters controlling the level of strength and ductility enhancement of over-reinforced HSC beams.
- The confinement in HSC beam had not any effect on the initial stiffness, where it had a significant effect on its ultimate capacity.
- The percentage of transverse bars is not the only factor that affects the performance of the beam but also the positions of the bars.
- In HSC beam, case of arranging the longitudinal bars in two rows, it could be better to put the number of bars in the second row half of the first row to gain best performance, more ductility and tensile force transferring.
- The yield and the ultimate strength of transverse reinforcement have a significant effect on the ultimate capacity of the HSC beam, which have to be considered in the confinement model of HSC beam.

REFERENCES

1. A. Azizinamini, S. Kuska, P. Brungardt and E. Hatfeild, "Seismic behavior of square high-strength concrete columns." *ACI J* 91 3 (1994), pp. 336–345.
2. A. Azizinamini, S.S. Baum Kuska, P. Brungardt and E. Hatfield, "Seismic behavior of square high-strength concrete columns". *ACI Struct J* 91 3 (1994), pp. 336–345.
3. A Elkader Haridy "Improving the flexural behaviour of over reinforced concrete beams" *M. Sc, Assiut university*, Egypt (2006).

4. A. K. Mohamed "Flexural behaviour of over reinforced helically confined concrete beams" *AL-AZHAR Engineering 9th international conf.* April (2007), pp. 512-525.
5. ACI 318-02, "Building code requirements for structural concrete", *American Concrete Institute* (2002).
6. ACI-ASCE Committee 441, "High-strength concrete columns": state of the art. *ACI Struct J* 94 3 (1997), pp. 325–335.
7. A.H. Mattock, L.B. Kriz and E. Hognestad, "Rectangular concrete stress distribution in ultimate strength design." *ACI J Proc* 57 8 (1961), pp. 875–928.
8. ANSYS User's *Manual, Version 9*, 2004
9. Egyptian code for design and construction of reinforced concrete structures (ECCS-203), Cairo (2007).
10. Hatanaka S, Tanigawa Y. "Lateral pressure requirements for compressive concrete." In: *Proceedings of 10th world conference on earth quake Engineering*, Madrid, (1992), p. 2603–8.
11. M.A. Mansur, M.S. Chin and T.H. Wee, "Flexural behavior of high-strength concrete beams", *ACI Struct J* 97 (6) (1997), pp. 663–674.
12. M.M. Ziara, D. Haldane and S. Hood, "Proposed changes to flexural design in BS 8110 to allow over-reinforced sections to fail in a ductile manner", *Mag Concr Res* 52 (6) (2000), pp. 443–454
13. M.N.S. Hadi and L.C. Schmidt, "Use of helixes in reinforced concrete beams", *ACI Struct J* 99 (2) (2002), pp. 304–314.
14. M.N.S. Hadi and N.M. Elbasha, "Effects of tensile reinforcement ratio and compressive strength on the behaviour of over reinforced helically confined HSC beams", *Construct Building Mater J* 21 (2) (2007), pp. 269–276.
15. Muhammad N.S. Hadi, and N. Elbasha "The effect of helical pitch on the behaviour of helically confined HSC beams" *Construction and building materials J*. Volume 22 (5), May (2008), pp. 771-780
16. N.M. Elbasha and M.N.S. Hadi, "Experimental testing of helically confined HSC beams", *Structural Concrete* 6 (2) (2005), pp. 43–48.
17. N.M. Newmark and W.J. Hall. In "Earthquake Spectra and Design", *Earthquake Engineering Research Institute*, Berkeley, Calif (1980), p. 103.
18. S.A. Sheikh, D.V. Shah and S.S. Khoury, "Confinement of high-strength concrete columns". *ACI J Proc 91 1 (1994)*, pp. 100–111.
19. S.A. Sheikh and S.M. Uzumeri, "Strength and ductility of tied concrete columns"*, J Struct* Div 106 (5) (1980), pp. 1079–1102.
20. S.K. Hwang and H. Doyun, "Effect of transverse reinforcement on flexural behaviour of high strength concrete columns", *Engineering structures J*. Volume 26 (1) January (2004), pp. 1-12.
21. S. Martinez, A.H. Nilson and F.O. Slate, Spirally reinforced high-strength concrete columns, *ACI Struct J* 81 (5) (1984), pp. 431–442.
22. S.W. Shin, S.K. Ghosh and J. Moreno, Flexural ductility of ultra-high strength concrete members, *ACI Struct J* 86 (4) (1989), pp. 394–400
23. Uniform Building Code. *International Conference of Building Officials*, Whittier, (1988),.
24. Y.K. Yong, M.G. Nour and E.G. Nawy, Behavior of laterally confined high-strength concrete under axial loads. *J Struct Eng ASCE* 114 2 (1988), pp. 332–351.

سلوك الانحناء للكمرات الخرسانية عالية المقاومة والمسلحة بنسبة حديد رئيسى عالى وكانات اضافية مستطيلة فى منطقة الضغط.

يتناول هذا البحث دراسة عملية ونظرية لمعرفة سلوك الانحناء فى الكمرات الخرسانية المسلحة بنسبة عالية من الحديد الرئيسى (بمنطقة الشد) ومحاطة بكانات اضافية مستطيلية الشكل بارتفاع نصف الكمرة (بمنطقة الضغط). حيث تمت الدراسة العملية باختبار اربعة كمرات طول كلا منها 2.2 متر وبارتفاع 23سم وثلاثة منها نسبة حديدها الرئيسى عالية وبها كانات اضافية فى منطقة الضغط وذات مقاومة خرسانية حدها الاقصى 500 كجم/سم2. وتم عمل دراسة نظرية وذلك بعمل موديل باستخدام طريقة العناصر المحددة وتم مقارنة نتائجة بنتائج الدراسة العملية وتبين درجة الدقة لهذا الموديل والذى تم استخدامه بعد ذلك لعمل دراسة لنفس النوع من الكمرات ولكن ذات مقاومة خرسانية عالية (تتراوح ما بين 600 الى 950 كجم/سم2) مع دراسة بعض المتغييرات مثل مقاومة الخرسانة وقطر الكانات الاضافية وقطر وعدد حديد التسليح الرئيسى واظهرت الدراسة مدى تاثير كل عنصر من العناصر السابقة على سلوك الانحناء لتلك النوع من الكمرات.